Combining Empirical Mode Decomposition with Independent Component Analysis for Single-Channel Signal Analysis

Bogdan Mijović, *Student Member, IEEE,* Joachim Taelman, *Student Member, IEEE,*
Ivan Gligorijević, and Sabine Van Huffel, *Fellow, IEEE*

Abstract

A method for decomposing a single-channel signal into its statistically independent components is proposed. This method combines Empirical Mode Decomposition (EMD) with Independent Component Analysis (ICA). Comparison is made with other algorithms for single channel signal decomposition such as Hankel Total Least Squares (HTLS), Single Channel ICA (SCICA), and a combination of Wavelets and ICA (WICA). Simulations show that the newly proposed method outperforms WICA and SCICA for high noise levels in extracting simple as well as complex oscillatory modes regardless of the shape. Performance of the new algorithm was also demonstrated on two real-life signal applications. The method showed to perform well on both stationary and non-stationary data and it was able to separate the independent sources having overlapping spectra. Both the shape and the amplitude of extracted signals was well recovered.

Index Terms

Empirical Mode Decomposition, Independent Component Analysis, Feature Extraction, Single Channel Signal Analysis, Blind Source Separation

I. Introduction

THE Empirical Mode Decomposition (EMD), proposed by Huang [1] is a novel signal analysis tool which is able to decompose any complicated time series into a set of spectrally independent oscillatory modes, called Intrinsic Mode Functions (IMFs). The advantage of EMD compared to Wavelet analysis is that EMD is able to deal with nonstationary and

All the authors are with the Department of Electrical Engineering (ESAT), division SCD, Katholieke Universiteit Leuven, 3001 Leuven, Belgium, e-mail: bogdan.mijovic@esat.kuleuven.be.

Manuscript received April 23, 2009.

nonlinear data. While wavelets and other signal decomposition techniques tend to map the signal space onto a space spanned by a predefined basis, EMD is a data driven algorithm which means that it decomposes the signal in a natural way where no a priori knowledge about the signal of interest embedded in the data series is needed.

On the other hand, *Independent Component Analysis* (ICA) is a well known and well established blind source separation (BSS) technique which can find statistically independent sources (components) from a set of recorded signals. However, this is possible only when the number of electrodes (channels) is larger than or equal to the number of sources. Unfortunately, with the single channel data this is possible only for the trivial case - where the number of sources is one, i.e. the signal is coming from only one source.

The extension of ICA to single channel signals, called Single Channel ICA (SCICA), has already been proposed by Davies and James [2]. However this technique has two major drawbacks: it is not able to deal with nonstationary data, and sources which are to be separated must have disjoint spectra.

The above-mentioned features of the EMD and ICA give us the possibility to overcome these drawbacks and lead us straightforwardly to the idea of joining the two methods in the following way: first, we decompose the signal using EMD into *spectrally independent* oscillatory modes (IMFs), and then perform ICA to the set of IMFs to extract *statistically independent* sources. Since the number of sources will be smaller than the number of signals (IMFs) this means that ICA will merge statistically dependent components into the same source. Afterwards, the signal can be easily reconstructed using only one or a limited set of sources of interest.

This newly proposed technique will allow extracting independent sources mixed up in the observed signal. A similar technique Wavelet-ICA (WICA) has been proposed in the literature [3], but it has almost never been used as a single-channel technique, and has never been applied to biomedical signals in this form. More often it has been applied to multi-channel signals, e.g. for extracting the ECG artefact from the EMG signal [4], making use of the corresponding ECG signal which has been recorded in parallel, or it has been used for separating the fetal ECG, from the mother ECG where 6 ECG channels were recording in parallel [5]. In these cases, the signal was first processed by an ICA algorithm applied to these channels, and after visual inspection, the sources containing the signal of interest are retained and the signal is back-reconstructed. The wavelets are then simply used for denoising. However, this assumes availability of the particular signal we want to extract or reject. In this paper we will use single-channel WICA for comparison with our algorithm. We will try to show that our technique outperforms the WICA algorithm, and has numerous advantages.

The paper is organized as follows. In section II, all the methods and algorithms used in this paper are shortly described. Next in section III we compare the performance of the described methods in a simulation set-up. Further on we will show the performance of the methods applied to the real-life examples in section IV, followed by a discussion and conclusion.

II. Methods

a) Ensemble EMD-ICA (EEMD-ICA): One of the major drawbacks of the EMD algorithm is that it is highly sensitive to noise. Therefore, we used in this paper a more robust, noise-assisted version of the EMD algorithm, called Ensemble EMD (EEMD), recently introduced by Huang [6]. The algorithm defines the IMF set for an ensemble of trials, each one obtained by applying EMD to the signal of interest with added independent, identically distributed white noise of the same standard deviation (SD). The ratio of the noise SD to the SD of the signal will be further referred to as a *noise parameter* (np).

Algorithm 1 EEMD-ICA

1. Add independent, identically distributed white noise of zero-mean and SD equal to np times the SD of the original signal.
2. Apply EMD to derive a set of IMFs (usually 10 to 15 IMFs) until the last IMF is a monotonic function or has at most one extremum.
3. Repeat steps 1 and 2 a number of times, resulting into an ensemble of IMF sets. A new noise sample is generated in each iteration.
4. Average over the ensemble to obtain a set of averaged IMFs
5. Perform the FastICA algorithm (or any other probabilistic ICA algorithm) on the obtained set of IMFs to extract sources and derive the corresponding mixing and unmixing matrices A and W
6. Select the source of interest and multiply it with mixing matrix A to back-reconstruct the appearance of those sources in the IMF set
7. Sum over all the newly derived IMFs to reconstruct the appearance of the source of interest in the original signal

The EEMD algorithm is available online at [7]. Taking into account properties of the white noise, we expect noisy components to be canceled out. In this work the np-value used was between 0.2 and 2.

After EEMD is performed and a set of averaged IMFs is derived, ICA is applied to the whole set of IMFs. The ICA algorithm used in this paper is the FastICA algorithm [8], [9], [10]. The detailed description of the EEMD-ICA algorithm is provided in Algorithm 1. It is worth noting that no IMF subset has been preselected as input of the ICA algorithm in order to keep this part of the algorithm as automatic as possible. We then select the independent component (IC) we are interested in. Note that this part has to be done by visual inspection unless some features of the signal of interest are known. In this work we knew exactly in which signal we were interested in, and therefore also this part has been completely automated. It is also worth emphasizing that the signal of interest was always embedded in only one of the IC's in the examples under study. The reconstruction of the signal is then straightforward. First we set all the other IC's to zero, then we multiply it with the mixing matrix to regenerate the IMF set, now containing only the component of interest, and then simply add all of them together to obtain the reconstructed signal.

b) Wavelets-ICA (WICA): Since the wavelet analysis is based on very similar ideas as the EMD, i.e. to decompose the signal into components of disjoint spectra, it was natural to compare the performance of the EEMD-ICA algorithm with the WICA algorithm. This algorithm is very similar to the one described above. First, the signal is decomposed into spectrally non-overlapping components using a wavelets decomposition. Then ICA is applied to the set of wavelet components and ICs are extracted. After selecting the ICs of interest, the signal is reconstructed. The algorithm is described as follows:

Algorithm 2 Wavelets-ICA (WICA)

1. Select the mother wavelet which is most similar with the source wanted to be extracted (in our case Daubechies 6)
2. Select the order of the Wavelet transform (in our case 8) and use the Wavelet decomposition to generate the input matrix for the ICA algorithm
3. Perform the FastICA algorithm (or any other probabilistic ICA algorithm) on the obtained set of IMFs to extract sources and derive the corresponding mixing and unmixing matrices A and W
4. Select the source of interest and multiply it with mixing matrix A to back-reconstruct the appearance of that source in the input matrix for ICA algorithm
5. Sum over all the rows of this matrix to back-reconstruct the appearance of the particular source in the original signal

Note, however, that in this case, the signal was always spread over a number of ICs for the examples under study, contrary to EEMD-ICA which could capture the signal of interest into one component only. The advantage of EEMD over wavelets is that EMD is able to deal with nonstationary data, and therefore we expect the EEMD-ICA algorithm to outperform WICA in this case. Additionally, EEMD has a data-driven, instead of a predefined basis, contrary to wavelets. For this study we chose the Daubechies 6 wavelet, since it showed the best performance. Similar conclusion holds for other wavelets.

c) SCICA: Single Channel ICA (SCICA) is the extension of the ICA algorithm to single-channel signals, first introduced by Davies and James [2], and is outlined in Algorithm 3.

The major drawbacks are that the algorithm assumes stationarity of the data, and that it is not able to separate components with overlapping spectra. The algorithm is discussed in detail in [2].

Algorithm 3 SCICA

1. First break up a time series $x(t)$ into a sequence of contiguous blocks $\mathbf{x}$, each having a length N, and treat them as a sequence of vector observations. Then form a matrix $\mathbf{X}$ as a set of observations $\mathbf{x}(k)$, $k = 1, 2, .., K$

$$\begin{aligned} \mathbf{x}(k) &= [x(k\tau), ..., x(k\tau + N - 1)]^{\mathrm{T}} \\ \mathbf{X} &= [\mathbf{x}(1), ..., \mathbf{x}(K)]^{\mathrm{T}} \end{aligned} \tag{1}$$

where k is the block index, τ is a time delay , and $(K\tau + N - 1)$ is the length of the original signal. Every row in the matrix $\mathbf{X}$ corresponds now to a single observation.

2. Apply the FastICA algorithm to this matrix, to derive the unmixing matrix $\mathbf{W}$ ($\mathbf{S} = \mathbf{WX}$, where $\mathbf{S}$ is a matrix containing row-wise the independent components).
3. Now the matrix $\mathbf{W}$ actually yields filters in its rows. Extract the particular source of interest simply by filtering the original signal $x(t)$ with the corresponding row of the matrix $\mathbf{W}$.
4. To extract the appearance of the source in the signal $x(t)$, weight the source and, if necessary multiply it by -1, because the ICA algorithm yields the matrix $\mathbf{W}$ with the accuracy up to multiplication by a constant. Since FastICA also provides the mixing matrix $\mathbf{A}$ as an inverse (or the pseudo-inverse if the number of sources and the number of channels differ) of $\mathbf{W}$ $\left(\mathbf{A} = \mathbf{W}^{-1}\right)$, we can simply multiply the extracted source $s(i)$ with the i-th column of the matrix $\mathbf{A}$ to obtain its appearance in the original signal.
5. Now subtract the appearance of the source $s(i)$ in the signal x, redefine this newly obtained signal as $x(t)$, and repeat the steps from 1 to 4 to further extract other sources from the new signal x obtained after this subtraction.

d) HTLS: The Hankel Total Least Squares (HTLS) method is proposed in [11], [12]. In contrast to the above-mentioned methods, HTLS is parametric and tries to model the signal as a sum of K exponentially damped sinusoids (EDS), as follows:

$$\begin{aligned} x(n) &= \sum_{k=1}^{K} a_k e^{-d_k} sin(2\pi f_k n\Delta t + \phi_k) + \varepsilon(n), \\ n &= 0, 1, ..., N - 1 \end{aligned} \tag{2}$$

where $j = \sqrt{-1}$, $n\Delta t$ is the time lapse between the origin and the sample $x(n)$, Δt is the sampling interval, $\varepsilon(n)$ is the residual, and N is equal to the number of data points. The parameters of this model are the amplitudes a_k, the phases ϕ_k, the damping factors d_k, and the frequencies f_k. The algorithm proceeds as in Algorithm 4

Since the model order is a priori unknown we need to estimate it. Several algorithms exist, like ESTimation ERror (ESTER) [13], and Subspace-based AutoMatic Order Selection (SAMOS). The latter one was shown to outperform the former one [14], and is used in this study. It exploits the shift-invariance property of the dominant subspace of the Hankel data matrix to estimate

Algorithm 4 HTLS

1. Arrange the data points $x(n)$, $n = 0, ..., N-1$ in a $(L \times M)$ - Hankel matrix H, $N = L + M - 1$, $L > 2K$.
2. Compute the singular value decomposition (SVD) of H
3. Truncate the SVD of H in order to obtain its best rank-$2K$ approximation.

$$H \approx \hat{H} = \hat{U}_{L\times 2K}\hat{\Sigma}_{2K\times 2K}\hat{V}^{\mathrm{H}}_{M\times 2K} \tag{3}$$

   here $\hat{V}^{\mathrm{H}}$ denotes the Hermitian transpose of matrix $\hat{V}$.

4. It can be shown that the matrix $\hat{U}$ satisfies the *shift invariance property* which means that we can form the following overdetermined set of equations

$$\hat{U}^{\uparrow} \approx \hat{U}_{\downarrow}\tilde{Z} \tag{4}$$

   where $\hat{U}^{\uparrow}$ and $\hat{U}_{\downarrow}$ are derived from $\hat{U}$ by omitting its first and last row respectively. Then compute an estimate of $\tilde{Z}$ by solving the above set of equations in total least squares sense. The $2K$ eigenvalues of $\tilde{Z}$ arise in conjugate pairs for real data, resulting into K signal poles $\tilde{z}_k = e^{-d_k} sin(2\pi f_k n\Delta t)$ from which the damping factors and frequencies can be derived.

5. Finally, substituting these frequencies and damping factor estimates into (2), results in a set of linear equations. Solving this set in least squares sense yields the estimated amplitudes a_k and phases ϕ_k.

the model order. The detailed derivation of the algorithm can be found in [14]. This algorithm is expected to perform best with signals which can be sufficiently well represented by the EDS model (as illustrated in section III-A1). Otherwise the performance will be degraded (as illustrated in section III-A2).

III. Simulations

In this section we provide two different types of simulations in order to show that our new method is able to separate different statistically independent sources from single-channel data in stationary as well as nonstationary circumstances and to compare the performance of the proposed method to that of the other available methods for single-channel data decomposition.

In the simulations we always mixed two signals: the signal we want to extract ($a(t)$), and another, unwanted signal which is considered to be noise ($b(t)$) in the following way

$$x_{\lambda}(t) = a(t) + \lambda b(t), \tag{5}$$

with $\lambda \in \mathbb{R}$ being a proportion factor, and $x_{\lambda}(t)$ being a mixed signal, i.e. an input to the algorithm. An important measure here is the *Noise Level* nl which is defined as follows [15]:

$$nl = \frac{RMS(\lambda \cdot b(t))}{RMS(a(t))}. \tag{6}$$

Changing λ alters the noise level of our simulated signals.

The aim of these simulations was to evaluate the performance of the proposed method and to compare it to other available methods. We performed several simulations for different noise levels going from 0.05 to 2 with steps of 0.05, for two different signal types, described below. The simulation performance is expressed in terms of the Relative Root Mean Squared Error (RRMSE):

$$RRMSE = \frac{RMS(a(t) - \hat{a}(t))}{RMS(a(t))} \cdot 100[\%], \tag{7}$$

where $\hat{a}(t)$ is the estimate of the signal of interest.

When applying the FastICA algorithm after EEMD or wavelets, the number of independent components to be extracted was set to 5 in the simulation section.

To evaluate the performance of the EEMD-ICA method in biomedical single-channel signal processing and to compare its performance in an objective way with the other available methods as outlined in section II (WICA, SCICA and HTLS), we executed the following two essentially different simulations. In III-A1 we try to extract the seizure event from a real-life background EEG signal contaminated by muscle artifact. In this case, the signal of interest is a stationary signal of oscillatory type which is representative for different physiological signals such as blood pressure, respiration, EEG α-rhythm, even heart rate series in some cases etc. In the second simulation, described in III-A2, we focus on the extraction of nonstationary, spike-like data. Hereto, an ECG artifact is chosen which needs to be extracted from a real-life EMG signal. Simply subtracting it from the original signal cleans up the EMG data. This spiky type of data is representative for a whole class of artifact removal problems such as extraction of the ECG artifact from other physiological signals like EEG, the extraction of interictal spikes in EEG signals, spiky type seizure detection in neonatal EEG [16], as well as spike detection in intracranial electroneural signals captured during deep brain recordings [17].

A. Simulations setup

1) Oscillation-type source extraction: To simulate the extraction of oscillation-type components, we consider here the extraction of an oscillatory seizure from EEG recordings. The EEG signal consists of awake background EEG activity from a normal subject contaminated by a muscle artifact. The muscle artifact was simulated by filtering white gaussian noise with a band-pass filter between 15 and $30Hz$. The simulated muscle artifact was superimposed on real-life background EEG. This

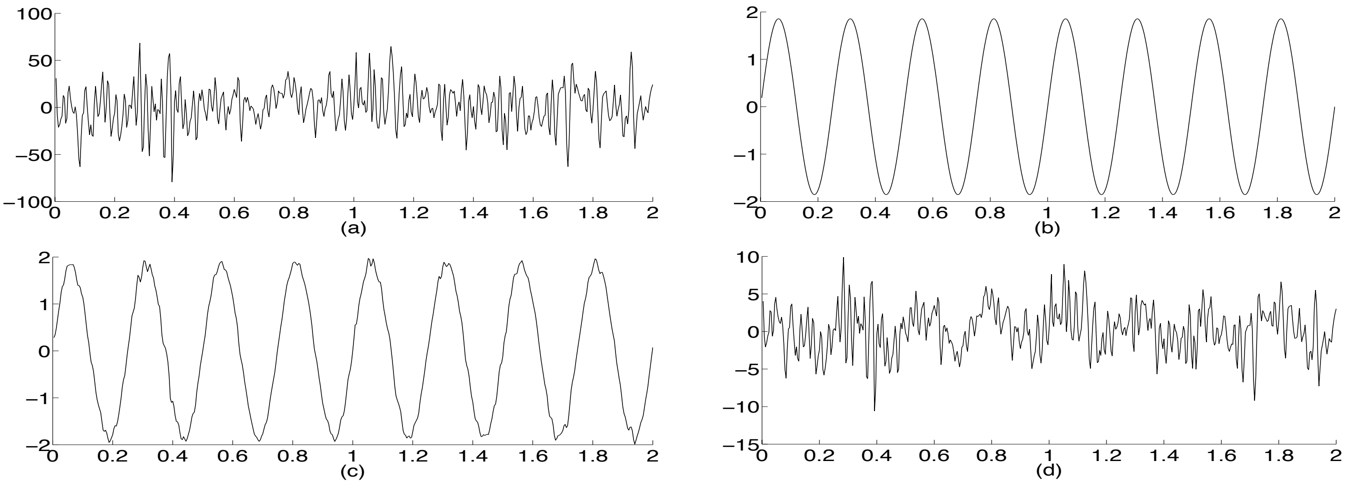

Fig. 1. (a) background EEG signal affected by muscle artifact used in the simulation, (b) Simulated seizure event, (c) Mixed signals for $nl = 0.05$, (d) Mixed signals for $nl = 2$

defines the noise part $b(t)$ in this simulation. The amplitude of the muscle artifact was chosen in a realistic way. Epileptic activity can be modeled in two ways - either as a spiky activity, or as a pure sinusoid. Here the epileptic activity was modeled as a $4Hz$ sinusoidal waveform (typical for patients having Mesial Temporal Lobe Epilepsy (MTLE) [18], [19]). Epileptic activity is in these simulations denoted as $a(t)$. Signals $a(t)$ and $b(t)$, as well as the mixed signals for different nl's are shown in figure 1.

2) Spike-type source extraction: To simulate the extraction of spiky-type sources, we mixed a pure real-life EMG signal (signal $b(t)$) with a simulated ECG artifact (signal $a(t)$) for different nl values, as described above. The ECG artifact signal was a real-life QRS complex repeated every 0.75 seconds, and zero padded in between. The mentioned peak is an artifact extracted from the EMG signal while no muscle activity was present. These signals are shown in figure 2. The frequency spectrum of the EMG signal is broad-band $(10 - 180Hz)$ with more or less equally distributed power over the whole range, while the ECG artifact is a narrow-band signal $(5 - 30Hz)$. Note that the spectra of the two signals are overlapping.

It is clear that the HTLS method will not be able to model these signals as a sum of EDS, and therefore the signal used for that simulation was shifted so that it doesn't start with an array of zeroes, but with one of the peaks, and only that part of the signal containing a single peak is modeled. This is depicted in figure 5.

B. Simulation Results and Discussion

Here we provide a comparison study. We show the performance of all the algorithms outlined in section II for nl going from 0.05 to 2, as mentioned before. The EEMD-ICA algorithm is performed for the level of np being 2. Additionally, we compare the performance of the EEMD-ICA algorithm for two different np values - 0.2 and 2 (figure 4). Figure 3 shows the

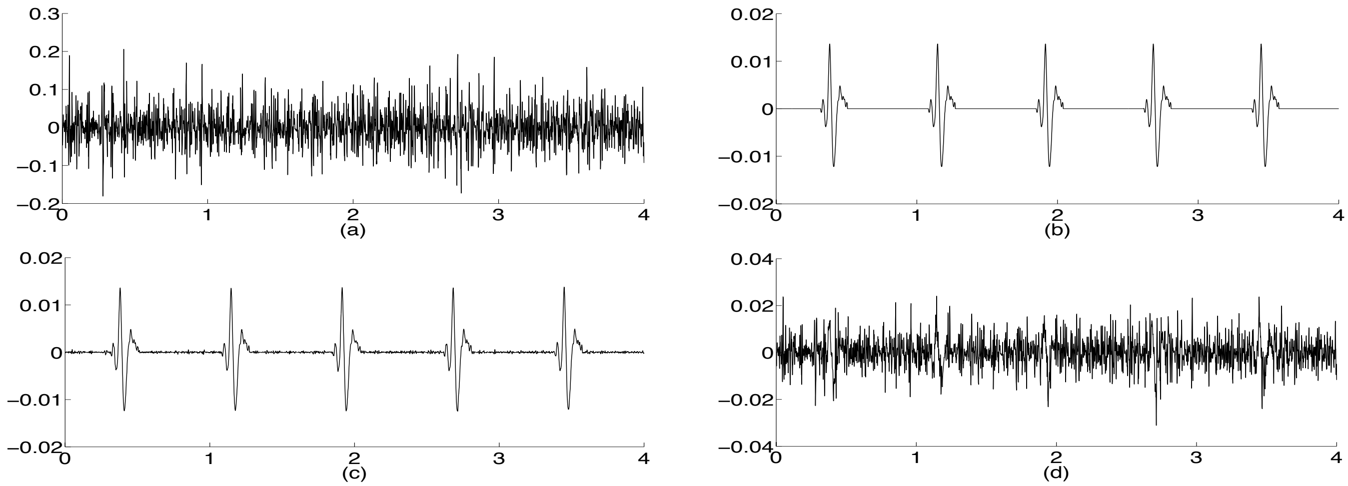

Fig. 2. (a) Pure EMG signal used in the simulation, (b) Simulated ECG artifact, (c) Mixed signals for $nl = 0.05$, (d) Mixed signals for $nl = 2$

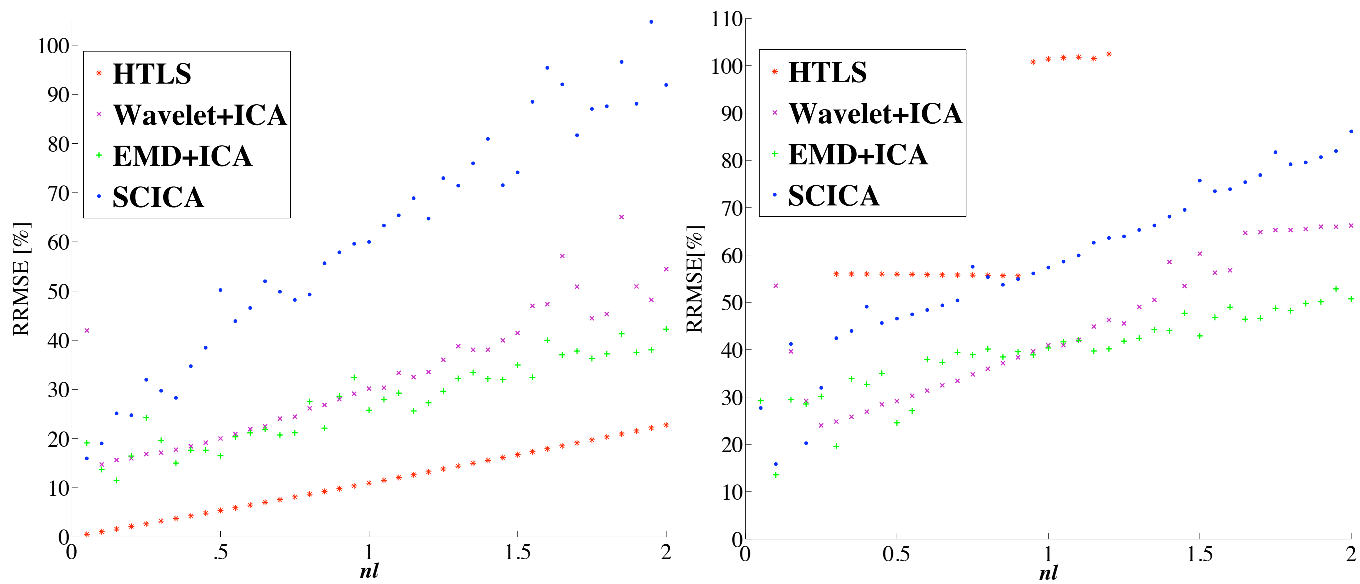

Fig. 3. Comparison of algorithms performances for the simulation described in III-A1 (left) and III-A2 (right)

performance of the 4 algorithms for the simulations in the sections III-A1 and III-A2 respectively.

From the left trace in figure 3, it is obvious that the HTLS method performs best for oscillatory-type source extraction. This is, of course, expected since the signal to be extracted is a pure sinusoid wave, and thus is easily modeled in this way. However, for the spiky-type source extraction simulation, HTLS is inferior to all the other algorithms for nl larger than 1 and lower than 0.3. This is due to the fact that for low nl, the algorithm cannot model the array of zeroes. When signal $b(t)$ is increased, HTLS can model the initial peak by a sum of sinusoids with large damping factor, see figure 5. Once nl is greater than 1, it starts modeling noise. This generates very high RRMSE, which can no longer be shown in the right trace in figure 3. The algorithm performance could be enhanced though, by specifying the model order a priori, given that we have some

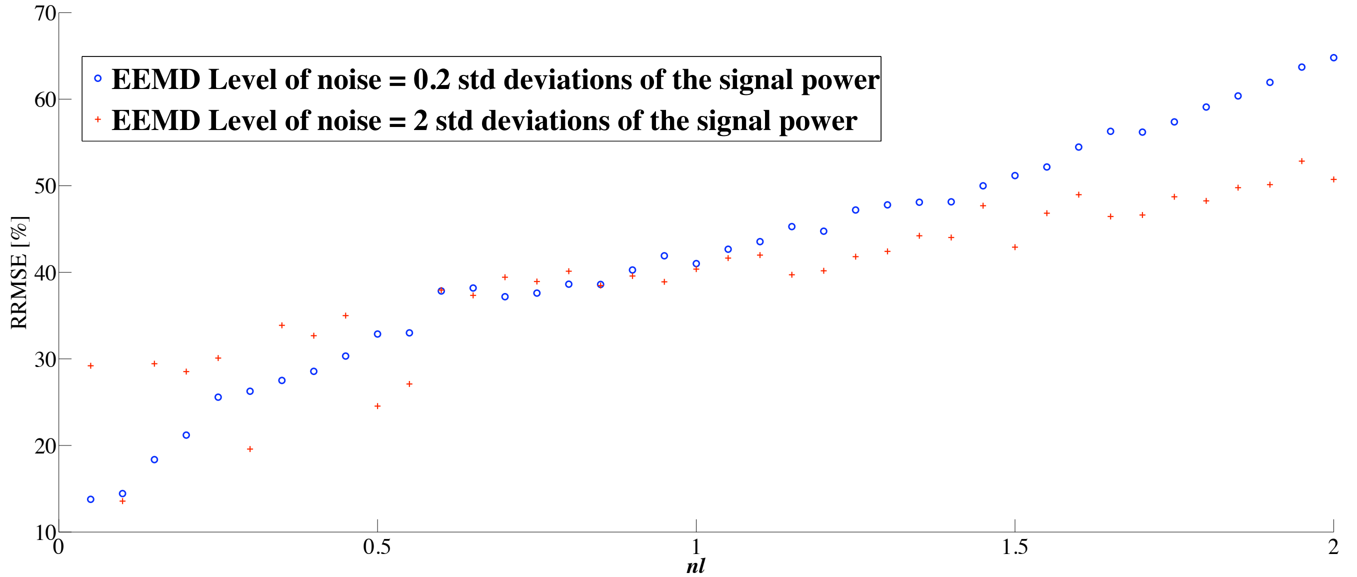

Fig. 4. Comparison of the EEMD-ICA algorithm for different levels of added noise

theoretical knowledge about the signal, instead of running the SAMOS algorithm to estimate it.

Compared to other algorithms, EEMD-ICA performs best for high noise levels, although it is not superior to WICA and SCICA for low noise levels. This is because too much noise is added for making an ensemble ($np = 2$), and the noise could not cancel out correctly. In figure 4, comparison is made between EEMD-ICA algorithms for different np-values (0.2 and 2). It is clear that the algorithm's performance depends on this factor, and that performance for low nl's can be enhanced by reducing it. This is a drawback of the EEMD-ICA algorithm in the sense that this parameter has to be chosen correctly in order to achieve the best performance. However, the EEMD-ICA algorithm outperformed WICA and SCICA in the spiky-type source extraction simulation for high nl values even when np is very low ($RRMSE = 50.73$ for $np = 2$, $RRMSE = 64.79$ for $np = 0.2$, and $RRMSE = 66.22$ for WICA). The best way to choose the np is to set it equal to the ratio of the SD of the noise already present in the signal and the SD of the signal itself. If no knowledge of the noise power is present either regular EMD technique might be used, or several np values could be tried out. However, the np should be smaller if the signal we want to extract has high frequency behavior and larger if the signal we want to extract is of low frequency content [6]. We would like to emphasize here that both the shape and the amplitude of the ECG artifact peak in the EMG simulation were almost perfectly recovered using the EEMD-ICA algorithm, contrary to the other methods, where the amplitude was mostly changed.

The SCICA algorithm performed clearly worse than other algorithms in the first simulation due to significant spectral overlapping of the data, although the data to be extracted was stationary. In the second simulation its performance was more

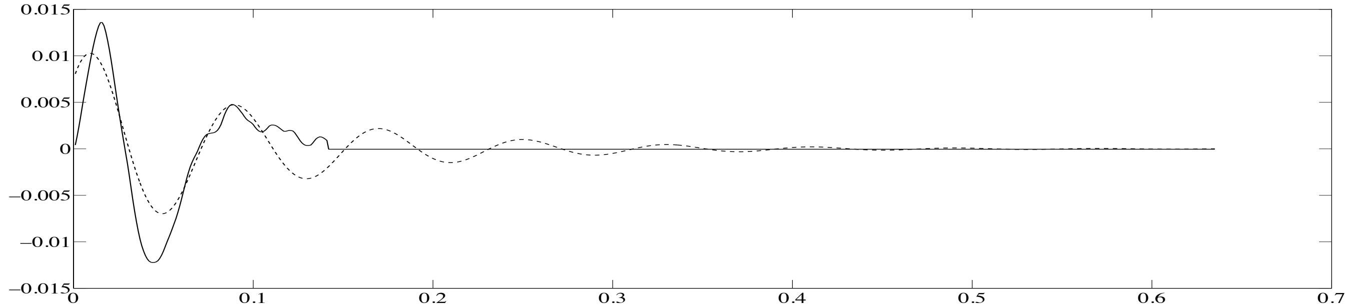

Fig. 5. ECG artifact for the EMG simulation (continuous line), and extracted signal using the HTLS method dashed line)

comparable to that of the other algorithms, however it was inferior to that of the EEMD-ICA algorithm due to the non-stationarity of the data this time.

IV. Real-life application of EEMD-ICA

To validate further the performance of the proposed algorithm, we applied the algorithm to real-life cases. We again consider two different cases. In the first case we apply the EEMD-ICA algorithm to one of the EEG channels contaminated by muscle artifact, eye artifact, and seizure activity. We try to separate this information into different sources. In the second case we will demonstrate how our new method performs in the case separating the ECG artifact from the EMG recordings, this time in-vivo. We showed in sections III-A2 and III-B that the algorithm showed very good performance in simulations. In the EEMD-ICA algorithm, the number of independent components to be extracted was set to 10 in the example IV-A1 because we were interested in 3 different sources and not all of them would appear in the first 5 IC's. In the example IV-A2, the number of IC's to be extracted was set to 5, as it was the case in section III. Here we will show how the EEMD-ICA algorithm with real-life signals.

A. Real-Life examples

1) EEG recordings: In figure 6, 10 seconds of 21-channel scalp EEG recordings from a long-term epilepsy monitoring unit are shown [15]. This recording contains ictal activity from a patient with MLTE, contaminated with eye blinks and muscle artifact. The sampling rate was $250Hz$. Since we consider here a single channel technique, we will apply EEMD-ICA only to the 21^{st} channel. Eye-artifacts can clearly be observed around 2.5, 3.5, 6 and 7.5 seconds, and are most emphasized in the 1^{st} and 12^{th} channel. Seizure activity is constantly present (20^{th} channel), and muscle activity starts on one side of the head (channels 13 to 21), and moves to the other side around the 5^{th} second (channels 1 to 8). We will try to extract all these artifacts from channel 21 by applying EEMD-ICA, as mentioned above which is more challenging since in this channel these artifacts are not so clearly visible.

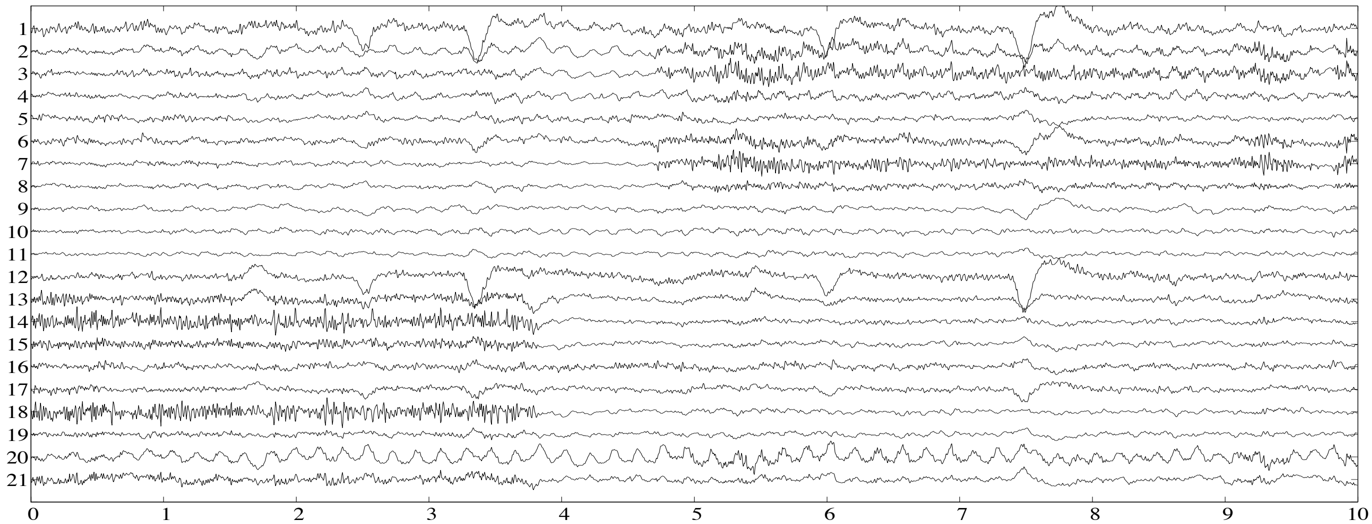

Fig. 6. 10 seconds of 21 channel EEG recordings

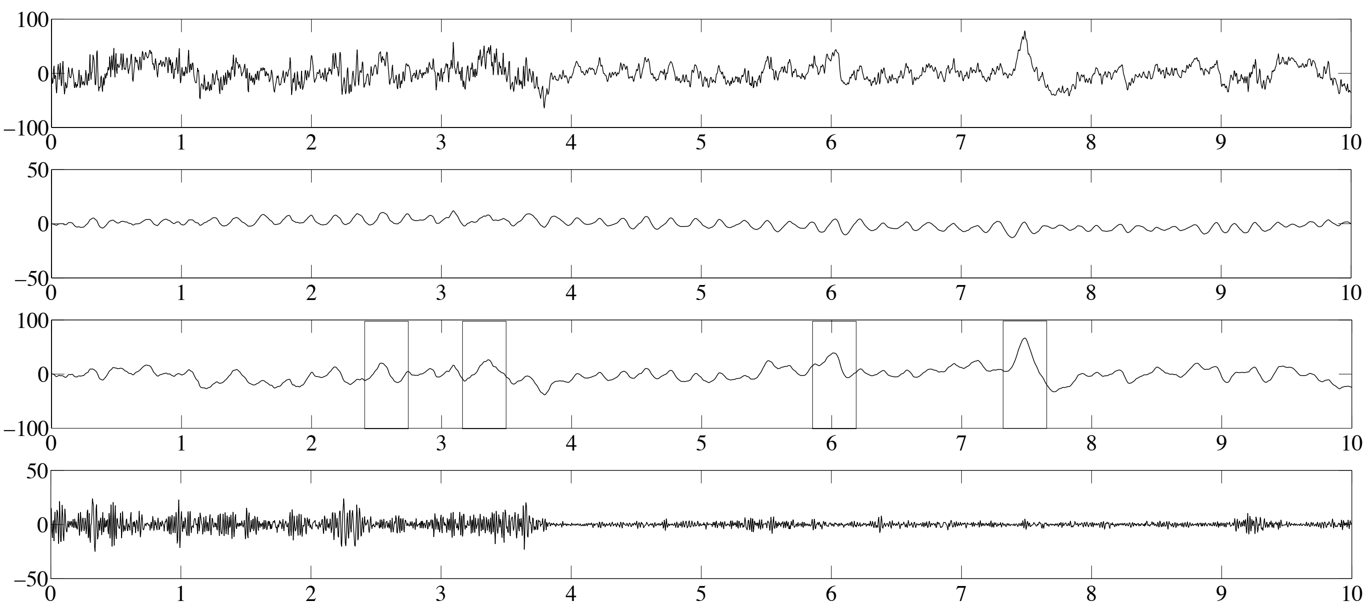

Fig. 7. 21^{st} EEG channel decomposed in the independent components. First row - original channel, second row - seizure event, third row - eye artifact (rectangles), fourth row - muscle activity

2) EMG recording: In the upper trace of figure 8 we give a recording of 100 seconds of the EMG signal contaminated with the ECG artifact. This recording corresponds to the phase immediately after the muscle activity, when the muscle is still not in the completely relaxed state. We chose this phase since the muscle activity is not so strong so the ECG artifact is visible, but the muscle is not in complete rest, so the power of the EMG signal is still fairly high. In the middle trace of this figure the extracted ECG artifact is shown, and the lower trace shows the cleaned EMG signal obtained by subtracting the extracted

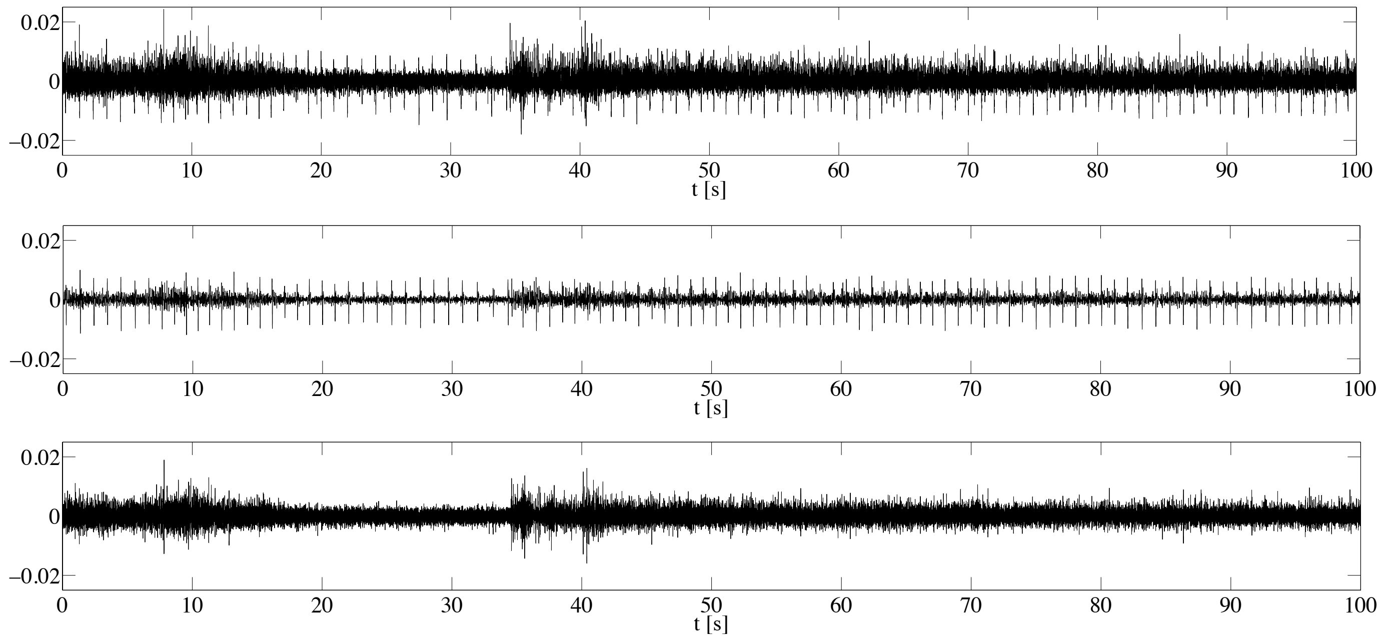

Fig. 8. EMG recording. Upper trace - original EMG signal, middle trace - extracted ECG artifact, lower trace - cleaned EMG signal. np was set to 0.5

artifact from the original signal.

B. Results and Discussion

Here we show results of applying our technique to the above-described examples, followed by a discussion. In figure 7, the 21^{st} channel of the EEG recordings is shown. After applying the EEMD-ICA algorithm, 11 independent components were extracted among which we chose 3 to back reconstruct the signals shown in the same figure, representing the seizure event, eye artifact and muscle activity respectively. We can clearly notice a successful extraction of the different components. The extracted seizure activity is in phase with the seizure activity visible in the 20^{th} channel, see figure 9. This confirms that this is really a seizure event and not any other oscillatory source. It is also clear that the eye artifact is more clearly expressed than in the original signal. Muscle activity is well separated.

Figure 8 shows the EMG signal contaminated by the ECG artifact. In the middle trace of this figure the extracted ECG artifact is shown, and the lower trace shows the cleaned EMG signal obtained by subtracting the extracted artifact from the original signal. Here we clearly see that the ECG artifact is nicely removed from the signal without distorting the original shape of the EMG signal. Here after applying the EEMD-ICA algorithm 4 sources were detected, only one of them containing the ECG artifact. The computed ratio of the standard deviation of the cleaned EMG signal to the standard deviation of the ECG artifact is 1, which is fairly high. The np in these applications was set to 0.5.

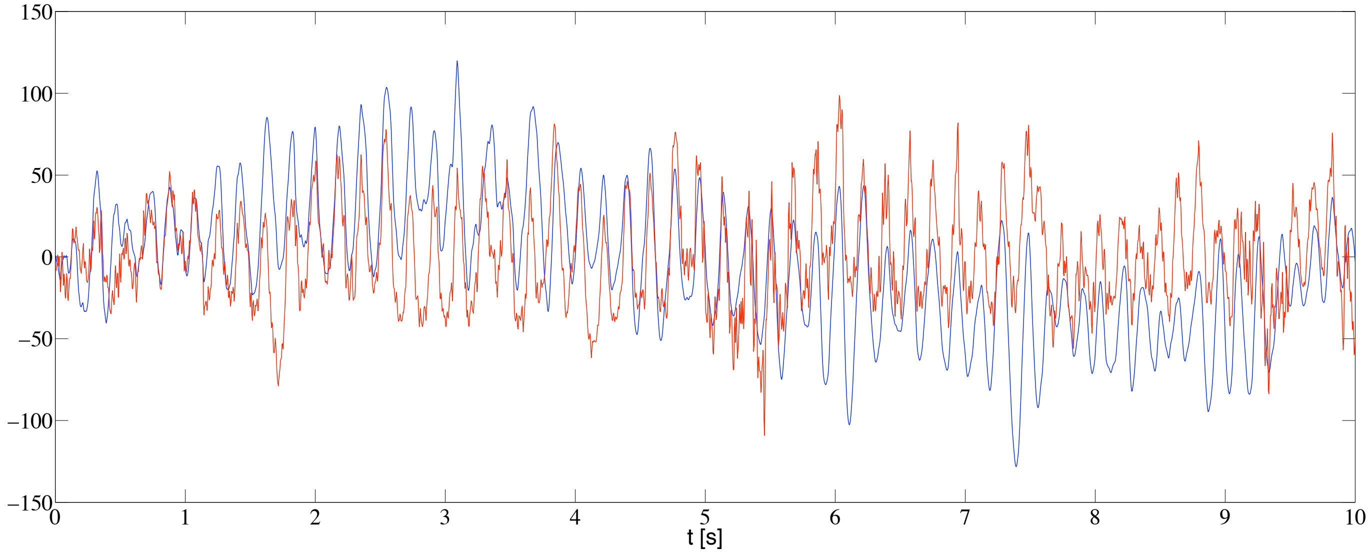

Fig. 9. Extracted seizure activity (blue) plotted against 20^{th} channel of the EEG recording (red). It is clear that the extracted activity is in phase with the activity from channel 20.

V. Conclusion

A new algorithm EEMD-ICA combining ensemble empirical mode decomposition with independent component analysis for single-channel signal decomposition was presented. We showed that it can deal with nonstationarity, and that it can separate two statistically independent signals having overlapping spectra. However, it is still not able to separate the signal from noise if both have similar statistical properties. Comparison with other algorithms for single-channel signal decomposition is made. The great advantage of the proposed algorithm over the WICA (combining wavelets with ICA) is that WICA has a predefined basis and is therefore not able to separate signals of different shapes from the signal in contrast to EEMD-ICA which extracts simple as well as complex oscillatory modes regardless of the shape.

From what is shown in this paper, the EEMD-ICA algorithm seems to be a promising tool for extracting independent sources from nonstationary data series. Afterwards different signal components may be separately back-reconstructed from the extracted sources, and may be helpful in better understanding and analysis of the data embedded in the signal. The extension of EEMD-ICA to multichannel signal decomposition is work in progress and will be discussed elsewhere.

Acknowledgment

Research supported by:

- Research Council KUL: GOA-AMBioRICS, CoE EF/05/006 Optimization in Engineering (OPTEC), IDO 05/010 EEG-fMRI, IOF-KP06/11 FunCopt, several PhD/postdoc & fellow grants;

- Flemish Government:
  - o FWO: PhD/postdoc grants, projects, G.0407.02 (support vector machines), G.0360.05 (EEG, Epileptic), G.0519.06 (Noninvasive brain oxygenation), FWO-G.0321.06 (Tensors/Spectral Analysis), G.0302.07 (SVM), G.0341.07 (Data fusion), research communities (ICCoS, ANMMM);
  - o IWT: TBM070713-Accelero, TBM-IOTA3, PhD Grants;
- Belgian Federal Science Policy Office IUAP P6/04 (DYSCO, 'Dynamical systems, control and optimization', 2007-2011);
- EU: BIOPATTERN (FP6-2002-IST 508803), ETUMOUR (FP6-2002-LIFESCIHEALTH 503094), Healthagents (IST200427214), FAST (FP6-MC-RTN-035801), Neuromath (COST-BM0601)
- ESA: Cardiovascular Control (Prodex-8 C90242)

REFERENCES

[1] N. E. Huang, M. L. Wu, S. R. Long, S. S. Shen, W. D. Qu, P. Gloersen, and K. L. Fan, "The empirical mode decomposition and the hilbert spectrum for nonlinear and non-stationary time series analysis," *Proc. Roy. Soc. Lond*, vol. 454A, no. 1971, pp. 903–993, 1998.

[2] M. E. Davies and C. J. James, "Source separation using single channel ica," *Signal Processing*, vol. 87, no. 8, pp. 1819 – 1832, 2007, independent Component Analysis and Blind Source Separation.

[3] J. Lin and A. Zhang, "Fault feature separation using wavelet-ica filter," *NDT & E International*, vol. 38, no. 6, pp. 421 – 427, 2005.

[4] B. Azzerboni, G. Finocchio, M. Ipsale, F. L. Foresta, and F. Morabito, "A new approach to detection of muscle activation by independent component analysis and wavelet transform," *Springer-Verlag, Lecture Notes in Computer Sciences*, vol. 2486, Sep. 2002.

[5] B. Azzerboni, F. L. Foresta, N. Mammone, and F. Morabito, "A new approach based on wavelet-ica algorithms for fetal electrocardiogram extraction," in *European Symposium on Artificial Neural Networks Bruges, ESANN-2005.*, Apr 2005, pp. 193–198.

[6] Z. Wu and N. E. Huang, "Ensemble empirical mode decomposition: a noise-assisted data analysis method," *Advances in Adaptive Data Analysis*, vol. 1, no. 1, pp. 1–41, 2009.

[7] http://rcada.ncu.edu.tw/research1_clip_program.html, "Ensembleemd algorithm."

[8] E. Moulines, J. F. Cardoso, and E. Gassiat, "Maximum likelihood for blind separation and deconvolution of noisy signals using mixture models," in *IEEE International Conference on Acoustics, Speech, and Signal Processing, ICASSP-97*, vol. 5, Apr 1997, pp. 3617–3620 vol.5.

[9] A. Hyvarinen and E. Oja, "Independent component analysis: algorithms and applications," *Neural Networks*, vol. 13, no. 4-5, pp. 411 – 430, 2000.

[10] http://www.cis.hut.fi/projects/ica/fastica/code/dlcode.shtml, "Fastica graphical user interface."

[11] S. Van Huffel, "Enhanced resolution based on minimum variance estimation and exponentioal data modeling," *Signal Processing*, vol. 33, no. 3, pp. 333–355, 1993.

[12] S. Van Huffel, C. Decanniere, H. Chen, and P. Van Hecke, "Algorithm for time-domain nmr data fitting based on total least squares," *Journal of Magnetic Resonance A*, vol. 110, no. 2, pp. 228–237, 1994.

[13] B. Roland, D. Bertrand, and R. Gael, "Selecting the modeling order for the esprit high resolution method: an alternative approach," in *IEEE International Conference on Acoustics, Speech, and Signal Processing, ICASSP-04*, vol. II, 2004, pp. 1025–1028.

[14] J. M. Papy, L. De Lathauwer, and S. Van Huffel, "A shift-invariance based model order selection technique," *IEEE signal processing letters*, vol. 14, no. 7, pp. 473–476, 2007.

[15] W. De Clercq, B. Vanrumste, J. M. Papy, W. Van Paesschen, and S. Van Huffel , "Modelling common ynamics in multichannel signals with application to artifact and background removal," *IEEE Transactions on Biomedical Engineering*, vol. 52, no. 12, pp. 2006–2015, 2005.

[16] W. Deburchgraeve, P. J. Cherian, M. De Vos, R. M. Swarte, J. H. Blok, G. H. Visser, P. Govaert, and S. Van Huffel, "Automated neonatal seizure detection mimicking a human observer reading eeg," *Clinical Neurophysiology*, vol. 119, no. 11, pp. 2447 – 2454, 2008.

[17] U. Rutishauser, E. M. Schuman, and A. N. Mamelak, "Online detection and sorting of extracellularly recorded action potentials in human medial temporal lobe recordings, in vivo," *Journal of Neuroscience Methods*, vol. 154, pp. 204–224, 2006.

[18] B. J. Fisch, *Generalized epileptiform patterns*, 3rd ed. Elsevier, 1999.

[19] ——, *Localized epileptiform patterns*, 3rd ed. Elsevier, 1999.